Simulation of macromolecule self-assembly in solution: a multiscale approach

PREPRINT

Atti del Convegno

"*Polymer Processing with Resulting Morphology and Properties: Feet in the Present and Eyes at the Future"*

Proceedings of the GT70 International Conference
Salerno, Italy, 15-17 October 2015

A.D., Di Pasquale N., Carbone P., Barresi A.A. and Marchisio L.D.
Simulation of macromolecule self-assembly in solution: a multiscale approach.

Paper S01-69

The paper has been published in
AIP Conference Proceedings 1695 (R. Pantani , V. Speranza, F. De Santis, eds.)
article nr. 020036

[ISBN 978-073541342-9; ISSN: 0094-243X, E-ISSN: 1551-7616; DOI: 10.1063/1.4937314]

Simulation of macromolecule self-assembly in solution: a multiscale approach

Alessio D. Lavino[1, a)], Nicodemo di Pasquale[2, b)], Paola Carbone[3, c)], Antonello A. Barresi[1 ,d)] and Daniele L. Marchisio[1, e)]

[1]*Dipartimento di Scienza Applicata e Tecnologia, Istituto di Ingegneria Chimica, Politecnico di Torino, C.so Duca degli Abruzzi 24, 10129 Torino, Italy.*
[2]*School of Chemistry, The University of Manchester, Oxford Road, Manchester M13 9PL, UnitedKingdom*.
[3]*School of Chemical Engineering and Analytical Science, The University of Manchester, Oxford Road, Manchester M13 9PL, UnitedKingdom.*

[a)]alessiodomenico.lavino@studenti.polito.it
[b)]nicodemo.dipasquale@manchester.ac.uk
[c)]paola.carbone@manchester.ac.uk
[d)]antonello.barresi@polito.it
[e)]corresponding author: daniele.marchisio@polito.it

Abstract. One of the most common processes to produce polymer nanoparticles is to induce self-assembly by using the solvent-displacement method, in which the polymer is dissolved in a "good" solvent and the solution is then mixed with an "anti-solvent". The polymer ability to self-assemble in solution is therefore determined by its structural and transport properties in solutions of the pure solvents and at the intermediate compositions. In this work, we focus on poly-ε-caprolactone (PCL) which is a biocompatible polymer that finds widespread application in the pharmaceutical and biomedical fields, performing simulation at three different scales using three different computational tools: full atomistic molecular dynamics (MD), population balance modeling (PBM) and computational fluid dynamics (CFD). Simulations consider PCL chains of different molecular weight in solution of pure acetone (good solvent), of pure water (anti-solvent) and their mixtures, and mixing at different rates and initial concentrations in a confined impinging jets mixer (CIJM). Our MD simulations reveal that the nano-structuring of one of the solvents in the mixture leads to an unexpected identical polymer structure irrespectively of the concentration of the two solvents. In particular, although in pure solvents the behavior of the polymer is, as expected, very different, at intermediate compositions, the PCL chain shows properties very similar to those found in pure acetone as a result of the clustering of the acetone molecules in the vicinity of the polymer chain. We derive an analytical expression to predict the polymer structural properties in solution at different solvent compositions and use it to formulate an aggregation kernel to describe the self-assembly in the CIJM via PBM and CFD. Simulations are eventually validated against experiments.

1. Introduction

Macromolecule self-assembly in solution has a wide spectrum of application, ranging from the production of pharmaceuticals[1] to the development of innovative processes in the food and personal care industries. All these fields have in common the use of a particular state of matter, the so-called soft matter. This particular state of matter is placed between the solid and liquid phase, leading to a wide range of properties and, consequently, to a wide range of applications.

A particular technique, called solvent-displacement, is often used to induce self-assembly: the polymer, poly-ε-caprolactone (PCL) in our case, is dissolved in a good solvent (i.e. acetone) and the solution is then mixed with a bad solvent, labeled anti-solvent, for the polymer (i.e. water) with which the solvent is fully miscible. These

processes are often conducted in small continuous mixers, such as Confined Impinging Jets Mixer[2] (CIJM), to control the conditions under which solvent and anti-solvent mix together.

The aim of this work is to develop a fully-predictive model, based on first-principles, and not tuned nor fitted on experimental data, in order to describe efficiently all the phenomena involved, namely the rapid initial mixing of the solvent and anti-solvent streams[3], the diffusion-controlled aggregation (or self-assembly) between polymer molecules that follows and the effect of turbulence, both on the mixing of the solvent and anti-solvent and on the self-assembly.

A population balance model (PBM) is necessary to describe the self-assembly of the polymer molecules into "soft" nanoparticles (or micelles) and to determine the cluster mass distribution (CMD). The rate with which polymer molecules self-assemble (or aggregate) is due to their radius of gyration and diffusion coefficient, determined in turn from full-atom Molecular Dynamics (MD) simulations. The PBM is linked with the continuum scale by implementing it into a computational fluid dynamics code, that is capable of describing the mixing of the solvent and anti-solvent streams.

2. Strategy for Multiscale Modelling

As said above, the strategy for multiscale modelling consists of studying three different scales: the molecular scale, with MD, to determine the configurational, structural and transport properties of the PCL molecules, the scale of the population of particles (or micelles or clusters), with PBM, to determine the CMD, and finally the continuum scale, with CFD, to determine the fluid dynamics within the CIJM.

The link within these three scales is depicted in Fig. 1. PBM and CFD are solved together in the same tool, namely CFD, by using the quadrature method of moments (QMOM)[4], whereas MD and PBM cannot be solved together, due to the large scale separation. In this case it is more convenient to use the parameter passing approach, in the form of a surrogate model. The information coming from MD is "fitted" with a surrogate model that describes how the radius of gyration of a single PCL molecule changes due to the composition of the solution (i.e. amount of solvent and anti-solvent). In this case the surrogate mode is the well-known Flory's law[5], which reads as follows:

$$\langle {R_g}^2 \rangle = k M_w^{2\nu} , \tag{1}$$

where ν is the Flory's exponent, k is the Flory characteristic ratio which considers the stiffness of the molecule, M_w is the molecular weight of the macromolecule and $\langle {R_g}^2 \rangle$ is the ensemble-averaged squared radius of gyration. To calculate the mean radius of gyration $\langle R_g \rangle$, the following approximation is made: $\langle R_g \rangle \cong \langle {R_g}^2 \rangle^{1/2}$.

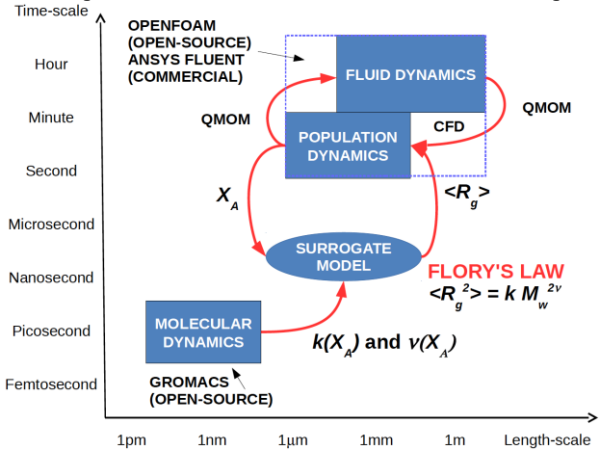

FIGURE 1. Representation of the three different scales investigated in this work.

3. Molecular dynamics

MD was used in this work to calculate the radius of gyration of a single PCL molecule (at three different molecular weights: $M_w = 1170, 2310, 3430$ gmol^{-1}) in a simulation box with different amounts of acetone and water, expressed in terms of the acetone molar fraction, x_A. MD simulations were performed by using the open-source code GROMACS and by employing the OPLS-AA force field for acetone and PCL and the SPC/E model for water. More details can be found in our recent work[6].

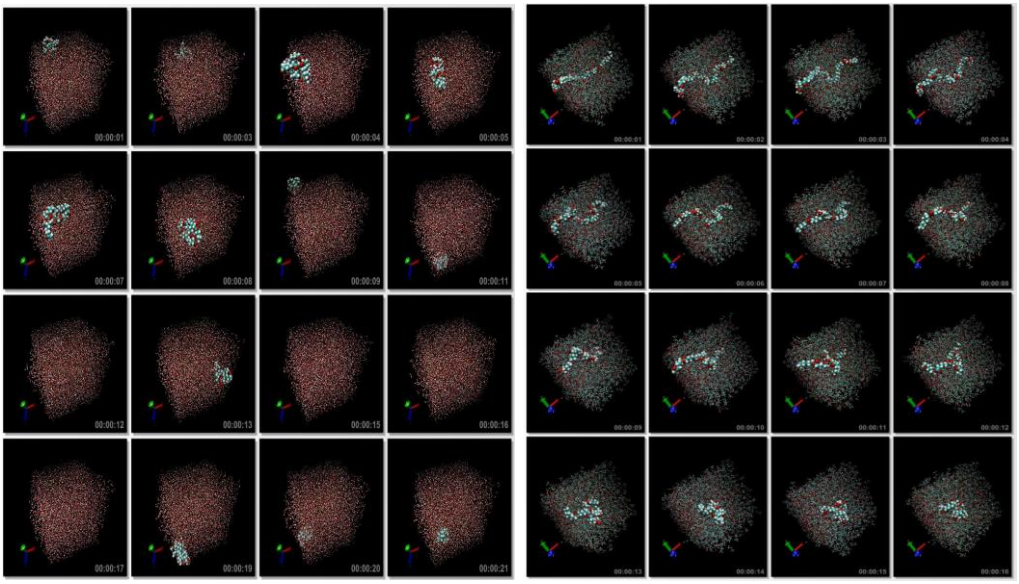

FIGURE 2. Temporal evolution of a PCL molecule with $M_w = 1170$ in pure water (left) and pure acetone (right) for about 20 ns.

Figure 2 shows the temporal evolution of a single PCL molecule in a simulation box composed of pure water and pure acetone. As it is seen in pure water the PCL is folded and very compact, due to the low affinity between PCL and water, resulting in very small values of the radius of gyration. On the contrary in pure acetone the PCL molecule is completely unfolded, resulting in large values of the radius of gyration. Surprisingly at intermediate compositions the PCL molecule behaves almost as in pure acetone, as the acetone molecules tend to cluster and surround the PCL molecule, which therefore "sees" a local environment very rich in acetone.

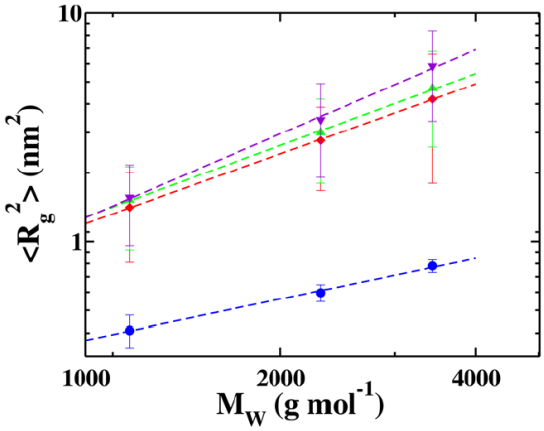

FIGURE 3. Squared radius of gyration of PCL molecules at different molecular weights in pure water $x_A = 0.00$ (blue line), pure acetone x_A=1.00 (purple line), $x_A = 0.75$ (green line) and $x_A = 0.50$ (red line).

Figure 3 clearly shows this effect, as the radius of gyration of PCL molecules for x_A=1.00, $0.75, 0.50$ is very similar, highlighting very little effect of the solution composition: as soon as some acetone is present in the solution the PCL molecule is stretched out and only in pure water the completely folded configuration is retrieved. If this data is fitted with the Flory's law of Eq. (1) (corresponding to the so-called "surrogate model") the following interpolating functions are obtained for the parameters k and ν:

$$k(x_A) = 0.0064 \exp(-3.15 x_A) \tag{2}$$

$$\nu(x_A) = 0.30 + 0.45 x_A - 0.15 x_A^2 \tag{3}$$

It is interesting to observe that the values of the Flory exponent ν obtained for pure water ($x_A = 0.00$) and pure acetone ($x_A = 1.00$) correspond to the theoretical values of 1/3 and 3/5, respectively, for a "bad" and a "good" solvent. This information, compacted into the surrogate model is then passed at the following scale (PBM).

4. Population dynamics

As mentioned PCL molecules self-assemble together forming nanoparticles and the dynamics of this population of particles is described with the PBM. The population is described here in term of the number of polymer molecules constituting one single nanoparticle: n. Since in the population of particles some particles are larger than others (and are therefore characterized by larger n values) a CMD is introduced: $f(n)$, representing the number of nanoparticles per unit volume of liquid mixture with n polymer molecules. Following the QMOM philosophy, only a few moments of the CMD are tracked: $m^{(k)} = \int f(n) n^k dn$ with $k = 0,1,2,3$. The moment of order zero represents the total number of nanoparticles, the moment of order one represents instead the total number of polymer molecules, whereas higher order moments are related to the variance and the skewness of the CMD.

Moreover, since the system is turbulent the CMD fluctuates around an average value, and being this flow with variable density (water and acetone have different densities), the Fauvre-average has to be used. The resulting Favre-averaged PBM, only accounting for polymer (and nanoparticle) aggregation reads as follows:

$$\frac{\partial}{\partial \boldsymbol{x}} \cdot \left(\bar{\rho} \langle \boldsymbol{U} \rangle \langle m^{(k)} \rangle (\boldsymbol{x}) \right) - \frac{\partial}{\partial \boldsymbol{x}} \cdot \left(\Gamma_t \frac{\partial}{\partial \boldsymbol{x}} \left(\langle m^{(k)} \rangle (\boldsymbol{x}) \right) \right) = \bar{\rho} \left\langle \frac{1}{2} \iint_0^{+\infty} \beta(n,n') \left(n^3 + n'^3 \right)^{\frac{k}{3}} f(n) f(n') dn dn' - \int_0^{+\infty} n^k f(n) \int_0^{+\infty} \beta(n,n') f(n') dn dn' \right\rangle \tag{4}$$

where the terms on the left-hand side represent convection and turbulent diffusion, whereas the terms on the right-hand side represent the appearance and disappearance of nanoparticles due to polymer molecule self-assembly. It is worth mentioning here that the PBM is very similar to the Boltzmann transport equation and the Smoluchovsky equation.

Closer inspection of Eq. (4) reveals that the equation is "unclosed": on the right-hand side only moments appear (which are global properties that belong to the continuum description), whereas on the left-hand side the CMD appears (that instead belong to the population dynamics description). The problem is closed by calculating the integrals appearing on the right-hand side with a quadrature approximation, which represents also a reconstruction of the CMD. More details on this method, called QMOM, can be found in the literature[4]. Moreover, another closure problem is present, due to the effect of turbulent fluctuations on the self-assembly dynamics. This second closure problem is closed by using the Direct Quadrature Method of Moments coupled with the Interaction and Exchange with the Mean (DMOM-IEM).

$\bar{\rho}$ is the Favre-averaged density, $\langle \boldsymbol{U} \rangle$ is the fluid mixture velocity (the system can be treated as pseudo-homogeneous thanks to very small Stokes number[7]), Γ_t is the turbulent diffusivity and β is the aggregation kernel, calculated as the summation of the Brownian[8]

$$\beta_{Br}(n,n') = \frac{2 k_B T}{3\mu} \frac{\left[\langle R_g \rangle (n) + \langle R_g \rangle (n') \right]^2}{\left[\langle R_g \rangle (n) \langle R_g \rangle (n') \right]}, \tag{5}$$

and turbulent shear kernels (under the condition of particle inertia negligible[9])

$$\beta_T(n,n') = 1.294\left(\frac{\epsilon\bar{\rho}}{\mu}\right)^{1/2}\left[\langle R_g\rangle(n) + \langle R_g\rangle(n')\right]^3, \tag{6}$$

where n and n' are the numbers of PCL molecules constituting the two colliding nanoparticles, μ is the dynamic viscosity of the acetone-water mixture, k_B is the Boltzmann constant, T is the systems temperature and ϵ is the turbulent dissipation rate. The radius of gyration of the colliding nanoparticles is calculated extending the Flory's law, valid for one PCL chain of molecular weight M_w, to a bundle of n PCL molecules of molecular weight M_w, as follows: $\langle R_g\rangle = \sqrt{k(nM_w)^2}$, following the freely jointed chain concept.

5. Continuum fluid dynamics

The third scale investigated is that of continuum fluid dynamics, via CFD, which simulates the mixing within the CIJM of the water and acetone streams. The equations that are solved are the Favre-averaged continuity equation and the Favre-averaged Navier-Stokes equation, which read as follows

$$\frac{\partial}{\partial \boldsymbol{x}}\cdot(\bar{\rho}\langle \boldsymbol{U}\rangle) = 0\,, \tag{7}$$

$$\frac{\partial}{\partial \boldsymbol{x}}\cdot(\bar{\rho}\langle \boldsymbol{U}\rangle\langle \boldsymbol{U}\rangle) = -\frac{\partial\langle p\rangle}{\partial \boldsymbol{x}} + \frac{\partial}{\partial \boldsymbol{x}}\cdot\left((\mu+\mu_T)\frac{\partial\langle \boldsymbol{U}\rangle}{\partial \boldsymbol{x}}\right), \tag{8}$$

where $\langle p\rangle$ is the Favre-averaged pressure, μ and μ_T are molecular and turbulent viscosity. As mentioned the CFD code is used to solve both the continuum fluid dynamics and the population dynamics scales. This is done by using the commercial CFD code Ansys/Fluent 15.0 on the entire CIJM geometry. This is constituted by two impinging jets mixing into a smaller cylinder chamber. A sketch of the simulated mixer is reported in Fig. 4.

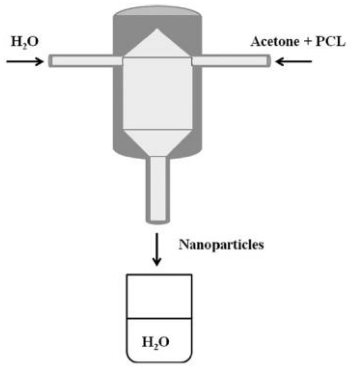

FIGURE 4. Sketch of the CIJM simulated in this work. The diameter of the inlet pipes is 1 mm, the chamber diameter and height are 5 and 11.2 mm, respectively.

The employed spatial numerical scheme is a first-order upwind scheme and the pressure–velocity coupling is solved with the SIMPLE algorithm. The standard k − ε turbulence model coupled with the Enhanced–Wall Treatment approach is used. Outlet boundary conditions assume zero normal gradients for all flow variables, except pressure, implying that outflow boundary values are not imposed but are calculated from the interior. The DQMOM-IEM and QMOM were implemented via User Defined Functions (UDF) in Fluent. Several concentrations and flow rates are investigated, as shown in Tab. 1. The flow rate ratio, *R*, between water and acetone is held equal to one. First, model predictions considering only polymer molecule self-assembly due to Brownian motions (i.e. Eq. (5)) was investigated; then also the effect of turbulent fluctuations (i.e. Eq. (6)) was considered.

TABLE 1. Operating conditions. For each flow rate all concentrations are investigated.

Flow rate, $\frac{mL}{min}$	PCL Concentration, $\frac{mg}{mL}$
10	0.50
20	2.5
40	5.0
60	10
80	15
120	25

Figure 5 shows contour plots of mean radius of gyration (in this case for Brownian aggregation only, as the trends are very similar when accounting also for turbulent aggregation). As it can be seen, the mean radius of gyration reaches its maximum values near the mixer walls, because the residence time in these regions is the highest, promoting extensive self-assembly. This figure clearly shows that in pure acetone stream (left side inlet) there is no aggregation (lower value of radius of gyration), because PCL molecules are stable in acetone and do not self-assemble. However, as soon as acetone and PCL molecules meet the water stream aggregation begins.

Closer observation of Fig. 5 reveals that by increasing the flow rate smaller nanoparticles are obtained.This is due by the fact that by increasing the flow rate, the mixing between acetone (and PCL) molecules and water molecules becomes more efficient, resulting in the formation of more PCL molecular clusters, that subsequently grow (through self-assembly) less.

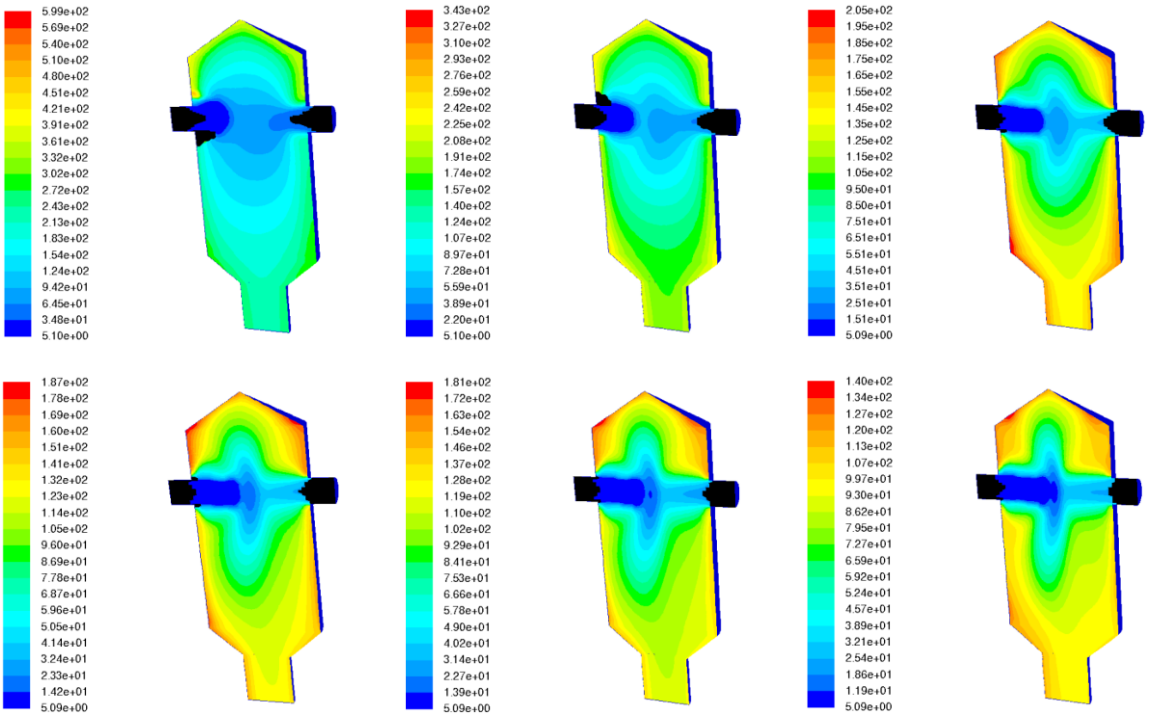

FIGURE 5. Contour plots of mean radius of gyration in the middle of the CIJM at an initial PCL concentration of 10 mg/mL^{-} From left to right and top to bottom the flow rates are 10, 20, 40, 60, 80 and 120 mL min^{-1}. The acetone and PCL inlet is on the left whereas the water inlet is on the right.

This is even more evident from Fig. 6 that reports the mean radius of gyration (measured with dynamic light scattering[10]) of the PCL nanoparticles at the outlet of the CIJM for different operating conditions (i.e. flow rates and initial PCL concentrations in the acetone stream). The continuous line is the predicted mean radius of gyration only

considering self-assembly induced by Brownian aggregation, namely induced by molecule fluctuations due to Brownian motions. The dashed lines considers instead together with this mechanism, also the self-assembly induced by turbulent fluctuations. As it is seen the agreement between the complete model (i.e. Brownian plus turbulent aggregation) is very good at higher initial polymer concentrations, whereas it is not satisfactory at the lowest concentrations investigated. This is probably due to the fact that the self-assembly mechanism considered here, namely diffusion-controlled aggregation, is only valid at high initial concentrations, whereas at low concentrations another mechanism, probably nucleative, kicks in.

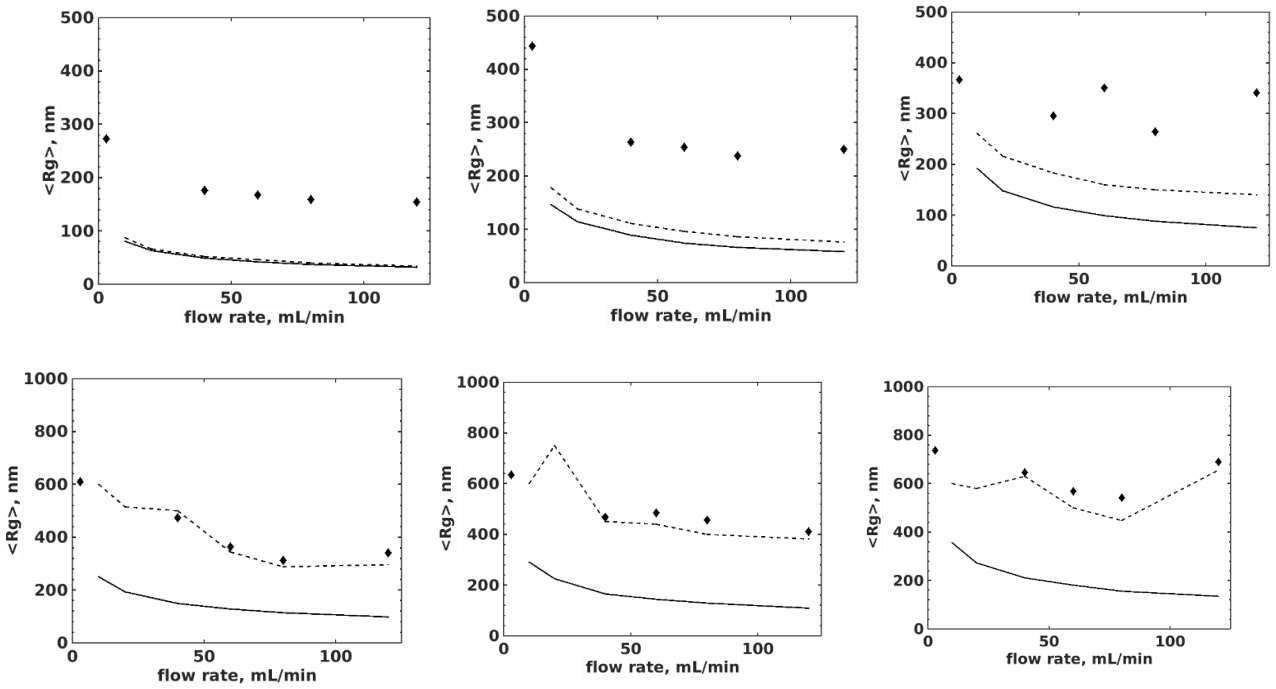

FIGURE 6. Comparison between experimentally measured mean radius of gyration of PCL nanoparticles (symbols), taken from our previous work[10], and model predictions considering the Brownian (continuous line) and Brownian plus turbulent (dashed line) self-assembly mechanisms at different flow rate values in the CIJM and different initial PCL concentrations in the acetone stream (from left to right and top to bottom: 0.5, 2.5, 5, 10, 15 and 25 mg mL^{-1}).

5. Conclusions

This work presents a new modelling approach to describe the self-assembly of PCL molecules into nanoparticles in water/acetone mixture. This new approach consists of a purely aggregative model (with Brownian and turbulent kernels), whose rate is estimated through the radius of gyration of the PCL molecules, evaluated in turn from MD. The results so obtained are then used in a coupled PBM-CFD approach to simulate a real process: PCL self-assembly induced by solvent-displacement in a CIJM under going turbulent mixing. Validation of model predictions is done in this work through comparison of the mean particle size, in terms of the mean radius of gyration, experimentally measured via dynamics light scattering in our previous work. Satisfactory agreement is found at high initial PCL concentrations, where probably the diffusion-controlled aggregation mechanism dominates the self-assembly, whereas pure agreement is detected at lower concentration, where other mechanisms might play a role.

REFERENCES

1. Wu, C., Jim, T.F., Gan, Z., Zhao, Y., Wang, S., **2000**. A heterogeneous catalytic kinetics for enzymatic biodegradation of poly(ε-caprolactone) nanoparticles in aqueous solution. Polymer 41, 3593.

2. Johnson, B.K., Prud'homme, R.K., **2003**. Chemical processing and micro-mixing in confined impinging jets. AIChE Journal 49, 2264.

3. Johnson, B.K., Prud'homme, R.K., **2003**. Flash nano-precipitation of organic actives and block copolymers using a confined impinging jets mixer. Australian Journal of Chemistry 56, 1021.

4. Marchisio, D.L., Fox, R.O. Computational models for polydisperse particulate and multiphase flows; Cambridge University Press: Cambridge, **2013.**

5. Rubinstein, M., Colby, R. H. Polymer Physics; Oxford University Press: New York, **2003**.

6. Di Pasquale N., Marchisio D.L., Barresi A.A., Carbone P. **2014**. Solvent structuring in water-acetone polycaprolactone mixtures and its effect on the polymer structure and processability. Journal of Physical Chemistry B. 118, 13258.

7. Baldyga, J., Orciuch, W., **2001**. Some hydrodynamic aspects of precipitation. Powder Technology 121, 9.

8. Smoluchowski, M., **1917**. Veruch einer Mathematischen Theorieder Koagulationskinetic Kolloider Lösungen. 11. Zeitschrift für Physikalische Chemie 92, 129.

9. Saffman, X., Turner, X., **1956**. On the collision of drops in turbulent clouds. Journal of Fluid Dynamics 47, 7202.

10. Lince F., Marchisio D.L., Barresi A.A., **2008**. Strategies to control the particle size distribution of poly-ε-caprolactone nanoparticles for pharmaceutical applications, Journal of Colloid and Interface Science 322, 505.